



日本原子力研究開発機構機関リポジトリ
Japan Atomic Energy Agency Institutional Repository

Title	Local- and intermediate-range order in room temperature superionic conducting Ag-GeSe ₃ glasses
Author(s)	Hosokawa Shinya, Kawakita Yukinobu, Stellhorn J. R., Pusztai L., Blanc N., Boudet N., Ikeda Kazutaka, Otomo Toshiya
Citation	JPS Conference Proceedings,33,p.011070_1-011070_7
Text Version	Published Journal Article
URL	https://jopss.jaea.go.jp/search/servlet/search?5068277
DOI	https://doi.org/10.7566/JPSCP.33.011070
Right	©2021 The Author(s) This article is published by the Physical Society of Japan under the terms of the Creative Commons Attribution 4.0 License. Any further distribution of this work must maintain attribution to the author(s) and the title of the article, journal citation, and DOI.

Local- and Intermediate-Range Order in Room Temperature Superionic Conducting Ag-GeSe₃ Glasses

Shinya HOSOKAWA,¹ Yukinobu KAWAKITA,² Jens Rüdiger STELLHORN,³ László PUSZTAI,^{4,5}
Nils BLANC,⁶ Nathalie BOUDET,⁶ Kazutaka IKEDA,⁷ Toshiya OTOMO⁷

¹Department of Physics, Kumamoto University, Kumamoto 860-8555, Japan

²J-PARC Center, Japan Atomic Energy Agency, Tokai 319-1195, Japan

³Department of Applied Chemistry, Hiroshima University Higashi-Hiroshima, 739-8527, Japan

⁴Wigner Research Centre for Physics, H-1525 Budapest, Hungary

⁵International Research Organization for Advanced Science and Technology, Kumamoto University, Kumamoto 860-8555, Japan

⁶Institut Néel, Centre National de la Recherche Scientifique (CNRS)/University of Grenoble Alpes, 38042 Grenoble Cedex 9, France

⁷High Energy Accelerator Research Organization (KEK), Tsukuba 305-0801, Japan

E-mail: shhosokawa@kumamoto-u.ac.jp

(Received January 8, 2020)

Local- and intermediate-range atomic order in Ag ion conducting glasses Ag_x(GeSe₃)_{1-x} with $x = 0.15, 0.28, 0.33,$ and 0.50 were investigated by combining anomalous X-ray scattering (AXS), X-ray and neutron diffraction (XRD and ND), and reverse Monte Carlo (RMC) modeling. By adding the ND pair distribution function to AXS and XRD results, reasonable partial structure factors and partial pair distribution functions were obtained. In contrast to the previous AXS and RMC study, significant Ag-Ge and Ge-Ge correlations are observed in the first coordination shell, which is consistent with an *ab initio* molecular dynamics simulation. The coordination numbers around the Ge and Se mostly follow the $8 - N$ rule over all Ag concentrations if Ag ions are not taken into account. With increasing the Ag concentration, the number of Ge and Se atoms around Ag increase remarkably, while the Ag-Ag coordination number increases only slightly. This indicates that the Ag conducting path is formed through the second neighbor Ag-Ag correlations.

KEYWORDS: Anomalous X-ray scattering, Neutron diffraction, Reverse Monte Carlo modeling, Glass structure

1. Introduction

Superionic conducting materials attract much attention in basic and applied materials science for electrolytes in solid-state batteries. Superionic behavior is observed in Ag containing chalcogenide glasses at room temperature, in contrast to crystalline superionic conductors that need high temperatures. In Ag_x(GeSe₃)_{1-x} glasses, an abrupt jump of about eight orders of magnitude is observed in the ionic conductivity at $x > 0.3$, where a superionic conducting phase is formed [1, 2]

For a wide range of Ag contents, the structural properties have been studied by Piarristeguy and co-workers by x-ray diffraction (XRD) [3, 4] and neutron diffraction (ND) [5]. A further structural investigation was carried out by the same group by ND and *ab initio* molecular dynamics (AIMD) simulation [6], where a strong evolution in the Ag-Ag correlations was observed in the Ag-Ag distance from the intermediate to short range with increasing the Ag concentration. Ohara and coworkers analyzed the structure by using high-energy XRD, ND, and EXAFS [7, 8]. ND experiments with Ag isotope enriched samples were carried out by Zeidler et al. [9, 10] to clarify the role of Ag atoms. Note that a strong phase separation tendency was reported in Refs. [6, 10] by electric force microscopy ob-

servations, which made the structural investigations more complex.

We measured anomalous X-ray scattering (AXS), analyzed by reverse Monte Carlo (RMC) modeling, for samples with $x = 0.50$ [11] and $x = 0.15$ and 0.50 [12]. All studies agree that the average coordination number of silver is remarkably high, reaching a value of three or more. Furthermore, chain-like fragments of Ag atoms can be clearly observed. Despite the large number of studies mentioned above, a detailed analysis of the intermediate range order (IRO) in Ag-GeSe₃ glasses is still missing.

From a recent work on the local structure of a metallic glass [13], it was found that a real space pair distribution function obtained by a total ND experiment, $g_N(r)$, gives useful information on the intermediate-range glass structures. In this study, ND experiments were carried out. Results were analyzed by RMC modeling again, to obtain more reliable and systematic information on Ag_x(GeSe₃)_{1-x} glasses with $x = 0.15, 0.28, 0.33,$ and 0.50 .

2. Experiments and data analysis procedures

Mixtures of pure elements were sealed in a quartz ampoule, which was heated using a furnace to 1050°C and kept for 12 h, followed by a quench in cold water.

The AXS experiments were carried out at the beamline BM02 of the ESRF, using incident beams of energies near the K edges of the constituent elements, i.e., 30 and 200 eV below the Ag K edge, and 20 and 200 eV below the Ge and Se K edges, to obtain differential structure factors, $\Delta_k S(Q)$, for each element. The principle and experimental procedure of AXS were given elsewhere [13–15].

ND experiments were carried out over a wide Q range, from 1.6 to over 1000 nm⁻¹, using the NOVA spectrometer [16] installed at BL21 of the MLF in J-PARC. The sample was contained in a standard cylindrical vanadium can with an outer diameter of 3 mm and a wall thickness of 0.1 mm. The proton beam power for generating neutrons was 500 MW. The ND experiment took 4 h for each sample, as well as for each calibration run. Scattered intensities from the sample were corrected for background, absorption by the sample and the cell [17], multiple [18], and incoherent scattering, by using the nvaSq software coded by the NOVA group [19].

RMC modeling [20] is a powerful tool for generating three-dimensional (3D) atomic configurations of disordered materials, on the sole basis of experimental diffraction data. The present RMC calculations were carried out by the RMC++ program package [21]. During the RMC procedure, the deviation between simulated and experimental structural data is minimized. Here, three differential structure factors, $\Delta_k S(Q)$ s, X-ray and neutron total scattering factors, $S_X(Q)$ and $S_N(Q)$, and $g_N(r)$ are applied. Number densities were obtained from the density measurements by Zeidler et al. [10]. Previous RMC calculations [11, 12] overestimated the number density by about 10%. Initial configurations were generated by hard-sphere Monte Carlo simulations. The simulation box contained 10,000 atoms in a size chosen to adjust the number density of the samples. From the 3D atomic configurations obtained by RMC modeling, partial structure factors, $S_{ij}(Q)$, and partial pair distribution functions, $g_{ij}(r)$, were computed.

3. Results

Fig. 1 shows experimental data of (a) $\Delta_{Ag} S(Q)$, (b) $\Delta_{Ge} S(Q)$, and (c) $\Delta_{Se} S(Q)$ obtained by AXS, and (d) $S_X(Q)$, (e) $S_N(Q)$, and (f) $g_N(r)$ for glasses with $x = 0.15, 0.28, 0.33,$ and 0.50 . The spectral features are very different from each other, owing to the different weighting factors for $S_{ij}(Q)$. In particular, $\Delta_{Ge} S(Q)$ has sharp pre-peak at about 10 nm⁻¹, and a deep minimum at about 20 nm⁻¹, where the prominent peaks are located in $S_X(Q)$ and $S_N(Q)$. On the other hand, $\Delta_{Se} S(Q)$ has a small prepeak and a large prominent peak. These features are very similar to those in $\Delta_{Ge} S(Q)$ and $\Delta_{Se} S(Q)$ of glassy GeSe₃ [14, 15]. When compared, the quality of RMC fits to $S_X(Q)$ and $S_N(Q)$ is slightly

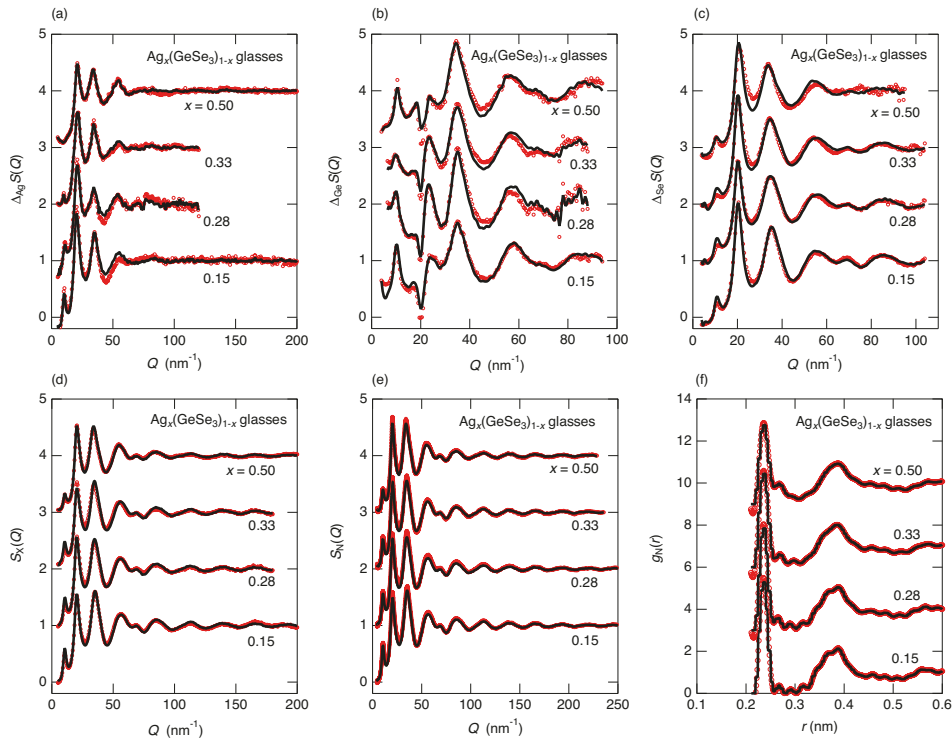


Fig. 1. (a) $\Delta_{\text{Ag}}S(Q)$, (b) $\Delta_{\text{Ge}}S(Q)$, (c) $\Delta_{\text{Se}}S(Q)$, (d) $S_X(Q)$, (e) $S_N(Q)$, and (f) $g_N(r)$ for glassy samples with $x = 0.15, 0.28, 0.33,$ and 0.50 , in the order from bottom to top. Circles: experimental data; solid curves: RMC fits. For clarity, the spectra are displaced.

better than that to $\Delta_k S(Q)$ s.

Figure 2 shows six $S_{ij}(Q)$ s as obtained from the RMC calculations for glassy samples with $x = 0.15, 0.28, 0.33,$ and 0.50 . Features of these functions highly depend on the combinations of elements. In the Ag-Ge, Ge-Ge, and Ge-Se partials, deep and sharp minima are seen at positions where the first peaks of experimental $S_X(Q)$ and $S_N(Q)$ are located (about 20 nm^{-1}), while the other partials have maxima there. As for the Ag concentration dependences, the obtained data in the low Q regions are not systematic, indicating that more reasonable $\Delta_{\text{Ag}}S(Q)$ data are necessary for a detailed discussion on the intermediate ordering around Ag atoms. All $S_{ij}(Q)$ s in the high Q region exhibit systematic changes with the Ag concentration, which suggests that short-range information, such as bond lengths and coordination numbers, is reliable.

Figure 3 shows all the six $g_{ij}(r)$ s as obtained from RMC calculations for glassy samples with $x = 0.15, 0.28, 0.33,$ and 0.50 . These $g_{ij}(r)$ functions are also quite different from each other. In the first coordination shell regions below 0.3 nm , the Ag-Ge, Ge-Ge, Ge-Se, and Se-Se correlations have prominent peaks, while the other Ag-Ag and Ag-Se partials have relatively small contributions. Note that the Ag-Ge and Ge-Ge contributions were not seen in the first coordination shells in the previous AXS and RMC study [11, 12], while an AIMD simulation [6] showed these contributions.

4. Discussion

To analyze the local atomic structures of $\text{Ag}_x(\text{GeSe}_3)_{1-x}$ conducting glasses in detail, numbers of neighbors of atom type j around type i element, N_{ij} (i.e. partial coordination numbers), were calculated from $g_{ij}(r)$ by integrating them up to $r = 0.30 \text{ nm}$. Total coordination numbers, N_i , were

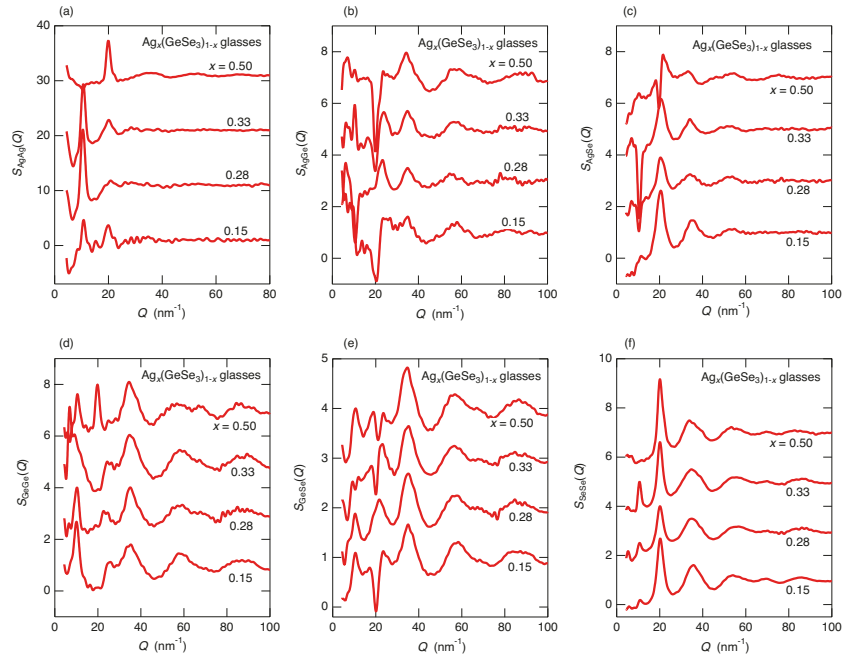


Fig. 2. $S_{ij}(Q)$ s of the (a) Ag-Ag, (b) Ag-Ge, (c) Ag-Se, (d) Ge-Ge, (e) Ge-Se, and (f) Se-Se correlations obtained from the RMC calculations for glasses with $x = 0.15, 0.28, 0.33,$ and 0.50 , in the order from bottom to top. For clarity, the spectra are displaced.

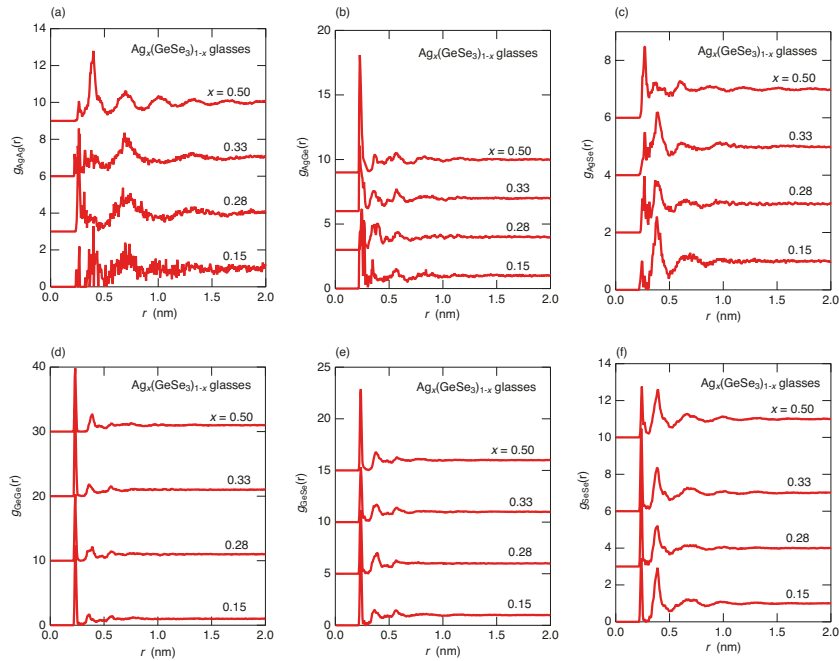


Fig. 3. $g_{ij}(r)$ s of the (a) Ag-Ag, (b) Ag-Ge, (c) Ag-Se, (d) Ge-Ge, (e) Ge-Se, and (f) Se-Se correlations obtained from the RMC calculations for amorphous samples with $x = 0.15, 0.28, 0.33,$ and 0.50 , in the order from bottom to top. For clarity, the spectra are displaced.

Table I. N_{ij} from the present study, together with previous experimental [8, 12] and theoretical [6] results.

x	Present				Experiments			Theory [6]		
	0.15	0.28	0.33	0.50	0.15 [12]	0.50 [12]	0.565 [8]	0.17	0.41	0.57
Ag-Ag	0.04	0.35	0.22	0.20	0.08	0.45	0.6	0.09	0.96	1.59
Ag-Ge	1.53	0.61	1.03	1.25	–	–	–			
Ag-Se	0.57	1.31	1.13	2.00	2.17	2.80	2.2	4.16	3.80	3.63
Ag total	2.14	2.27	2.38	3.45	2.25	3.25	2.8			
Ge-Ag	0.27	0.24	0.51	1.25	–	–	–	0.10	0.26	0.25
Ge-Ge	1.32	0.94	1.35	0.79	–	–	–	0.25	0.17	0.16
Ge-Se	2.76	2.20	2.15	2.45	4.07	3.98	3.7	3.37	3.23	3.30
Ge total	4.35	3.38	4.01	4.49	4.07	3.98	3.7			
Se-Ag	0.03	0.17	0.19	0.67	0.13	0.93	0.9			
Se-Ge	0.92	0.74	0.72	0.82	1.36	1.33	1.2			
Se-Se	1.17	1.67	1.64	1.05	0.78	0.65	–	1.05	0.78	0.54
Se total	2.12	2.58	2.55	2.54	2.26	2.91	2.1			

also calculated around element i . Results are tabulated in Table I together with previous experimental [8, 12] and theoretical [6] findings.

The present N_{ij} values are, in general, in good agreement with those from previous experimental work [8, 12]. However, the distinct Ag-Ge and Ge-Ge correlations are observed here, while these contributions were intentionally excluded during previous experimental studies, by imposing constraints on closest approaches in the RMC calculations. The exclusion of these contributions highly degrade the quality of RMC fits, particularly to the new ND data.

A remarkable difference from AIMD results [6] appears in Ag-related N_{ij} s: according to AIMD, N_{AgAg} increases significantly with increasing Ag concentration. It was also concluded there that direct connections between Ag atoms may be the origin of superionic conduction. Present results, as well as preceding experimental work, on the other hand, indicate only a small increase of N_{AgAg} . In contrast, increasing Ag fraction here brings about a large increase of the number of Ag atoms in the second coordination shell, at around 0.42 nm, as shown in Fig. 3(a). In parallel, N_{GeAg} and N_{SeAg} also increase, as shown in Table I. Thus, it may be concluded that the Ag ionic conducting path is formed through the second neighboring Ag-Ag correlations.

To clarify this speculation in more realistic, 3D atomic representations are displayed in Fig. 4 for glasses with $x = 0.15, 0.28, 0.33,$ and 0.50 , obtained from the present RMC calculations. Since the superionic conduction suddenly appears at the Ag concentration of $x = 0.3$ [1, 2], a percolation may happen for the conducting path of the Ag ions. For this, a direct Ag-Ag correlation is usually considered for the percolation mechanism [6]. However, the Ag-Ag direct connections are sparse in the atomic configurations obtained experimentally even for the glass with $x = 0.50$ as shown in Fig. 3 of Ref. [11] and Fig. 5(b) of Ref. [12].

Bars in Fig. 4 represent the Ag-Ag correlation on the level of the second coordination shell up to $r = 0.52$ nm. From the viewpoint of the percolation, the Ag-Ag path looks isolated or terminated for glasses with $x = 0.15$ and 0.28 (see Fig. 4(a) and (b)). On the other hand, the path starts to percolate in the glassy system with $x = 0.33$ (see Fig. 4(c)), and highly expands over the system with $x = 0.50$ (see Fig. 4(d)). Hence, it is concluded that the percolation path should include the second shell level of the Ag-Ag correlation in the sense of static structures of the Ag-GeSe₃ superionic glasses. If such a percolation path is formed, Ag atoms would easily travel by switching the first and second neighboring connections in the glasses.

Concerning elements of host network, Ge and Se, a large number of Ge-Ge and Se-Se bonds are observed, while the number of the heteropolar Ge-Se bonds is rather small compared with the host

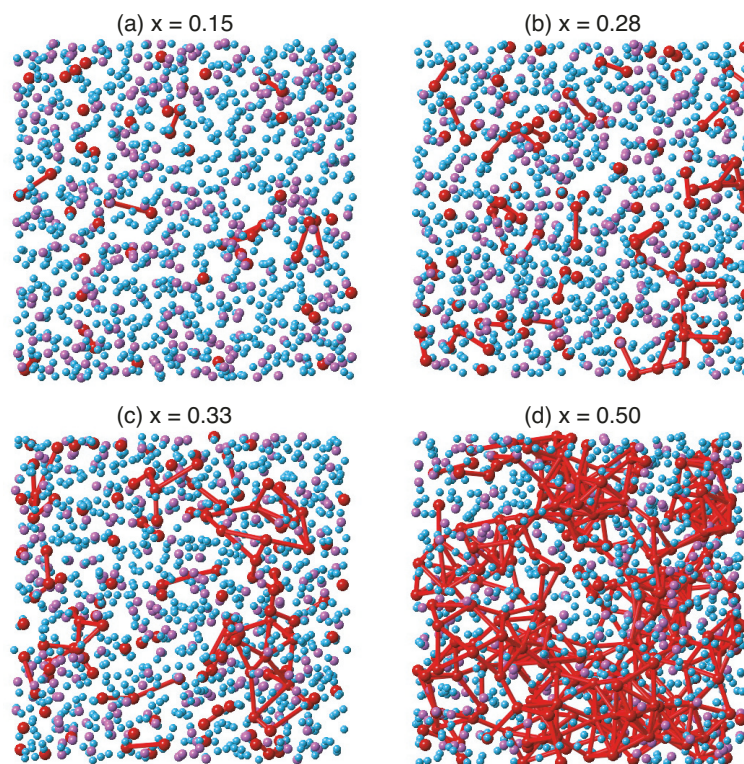


Fig. 4. 3D atomic representations for glasses with $x = 0.15, 0.28, 0.33,$ and 0.50 in the order from (a) to (d), obtained from the RMC calculations. Large, middle, and small balls indicate the Ag, Ge, and Se atoms, respectively, and the bars represent the Ag-Ag correlation on the level of the second coordination shell up to $r = 0.52$ nm.

GeSe₃ value [15]. This may reflect a tendency for some kind of 'phase separation' at a microscopic scale, which tendency was also found macroscopically by electric force microscopy [6, 10].

In the present study, N_{Se} largely exceeds two (c.f. Table I), the value that would be expected from the $8 - N$ rule; this is in agreement with previous experimental data [8, 12]. If N_{Se} is calculated by excluding Ag atoms, the picture changes dramatically: N_{Se} for the Ge-Se covalent network become much closer to two (see Table I), the value belonging to the $8 - N$ rule. N_{Ge} values approach four, which is expected from the $8 - N$ rule, if the Ag contributions are excluded. It may then be suggested that Ag atoms occupy interstitial positions in the host Ge-Se network. The addition of Ag atoms seems to trigger the increase of the number of Ge-Ge and Se-Se homopolar wrong bonds.

These features of the glass structures may give a hint why the superionic nature is realized at room temperature in the glasses, in conflict with superionic crystals. Owing to the structural periodicity in crystals, Ag atoms should always overcome an energy barrier formed by surrounding non-Ag atoms, and a high temperature is necessary for escaping such cages. Due to the random configurations and phase-separation tendencies in the glasses, Ag atoms can easily conduct by selecting low energy-barrier directions even at room temperature.

5. Summary

Local- and intermediate-range order in Ag_x(GeSe₃)_{1-x} glasses were investigated by combining AXS, XRD, ND experiments and RMC modeling. In contrast to the previous AXS and RMC study, a large number of Ag-Ge and Ge-Ge correlations are observed in the first coordination shell region,

which is consistent with a recent AIMD simulation. N_{Ge} and N_{Se} values follow the $8 - N$ rule if Ag atoms are not taken into account. With increasing the Ag concentration, N_{AgGe} and N_{AgSe} values increase remarkably, while N_{AgAg} increases only slightly. This indicates that the Ag conducting path is formed by the second neighboring Ag-Ag correlations. As mentioned above, the atomic configurations are reliable in the first shell region, while the second neighboring structures do not show a systematic change with the Ag concentration. To improve the quality of the structural information further, more verified AXS data, $\Delta_{\text{Ag}}S(Q)$ in particular, would be necessary for correctly identifying ion conducting paths in these glasses.

Acknowledgments

ND measurements were performed at BL21 of MLF/J-PARC (Proposal No. 2018B0299). AXS experiments were carried out at BM02 of the ESRF (Nos. HD 540 and HC1137). Supporting AXS experiments were performed at BL13XU of the SPring-8 (No. 2014A1060). This work was partly supported by Japan Science and Technology Agency (JST) CREST (No. JPMJCR1861), and the Deutsche Forschungsgemeinschaft (DFG) Mercator Fellowship in FOR 2824.

References

- [1] M. Kawasaki, J. Kawamura, Y. Nakamura, and M. Aniya, *Solid State Ionics* **123**, 259 (1999).
- [2] A. Piarristeguy, J. M. Conde Garrido, M. A. Ureña, M. Fontana, and B. Arcondo, *J. Non-Cryst. Solids* **353**, 3314 (2007).
- [3] A. Piarristeguy, M. Mirandou, M. Fontana, and B. Arcondo, *J. Non-Cryst. Solids* **273**, 30 (2000).
- [4] A. Piarristeguy, M. Fontana, and B. Arcondo, *J. Non-Cryst. Solids* **332**, 1 (2003).
- [5] G. J. Cuello, A. Piarristeguy, A. Fernández-Martínez, *J. Non-Cryst. Solids* **353**, 729 (2007).
- [6] A. A. Piarristeguy, G. J. Cuello, A. Fernández-Martínez, V. Cristiglio, M. Johnson M. Ribes, and A. Pradel, *Phys. Status Solidi B* **249**, 2028 (2012).
- [7] K. Ohara, L. S. R. Kumara, Y. Kawakita, S. Kohara, M. Hidaka, and S. Takeda, *J. Phys. Soc. Jpn.* **79**, Suppl. A 141 (2010).
- [8] L. S. R. Kumara, K. Ohara, Y. Kawakita, S. Kohara, P. Jónvári, M. Hidaka, N. E. Sung, B. Beuneu, and S. Takeda, *Eur. Phys. J. Web Conf.* **15**, 02007 (2011).
- [9] A. Zeidler, P. S. Salmon, A. Piarristeguy, A. Pradel, and H. E. Fischer, *Z. Phys. Chem.* **230**, 417 (2016).
- [10] A. Zeidler, P. S. Salmon, D. A. J. Whittaker, A. Piarristeguy, A. Pradel, H. E. Fischer, C. J. Benmore, and O. Guibiten, *R. Soc. open sci.* **5**, 171401 (2018).
- [11] J. R. Stellhorn, S. Hosokawa, Y. Kawakita, D. Gies, W.-C. Pilgrim, K. Hayashi, K. Ohoyama, N. Blanc, and N. Boudet, *J. Non-Cryst. Solids* **431**, 68-71 (2016).
- [12] J. R. Stellhorn, S. Hosokawa, W.-C. Pilgrim, Y. Kawakita, K. Kamimura, K. Kimura, N. Blanc, and N. Boudet, *Z. Phys. Chem.* **230**, 369 (2016).
- [13] S. Hosokawa, J.-F. Bérrar, N. Boudet, W.-C. Pilgrim, László Pusztai, S. Hiroi, K. Maruyama, S. Kohara, H. Kato, H. E. Fischer, and A. Zeidler, *Phys. Rev. B* **100**, 054204 (2019).
- [14] S. Hosokawa, Y. Wang, J.-F. Bérrar, J. Greif, W.-C. Pilgrim, and K. Murase, *Z. Phys. Chem.* **216**, 1219 (2002).
- [15] S. Hosokawa, I. Oh, M. Sakurai, W.-C. Pilgrim, N. Boudet, J.-F. Bérrar, and S. Kohara, *Phys. Rev. B* **84**, 014201 (2011).
- [16] https://j-parc.jp/researcher/MatLife/en/instrumentation/ns_spec.html#bl21, (2019).
- [17] H. H. Paalman and C. J. Pings, *J. Appl. Phys.* **33**, 2635 (1962).
- [18] I. A. Blech and B. L. Averbach, *Phys. Rev.* **137**, A1113 (1965).
- [19] <http://research.kek.jp/group/hydrogen/analysis.html>, (2015).
- [20] R. L. McGreevy and L. Pusztai, *Molec. Simul.* **1**, 359 (1988).
- [21] O. Gereben, P. Jónvári, L. Temleitner, and L. Pusztai, *J. Optoelectron. Adv. Mater.* **9**, 3021 (2007).